Available online at www.sciencedirect.com
SCIENCE DIRECT®
Microelectronic Engineering 75 (2004) 423–432
MICROELECTRONIC ENGINEERING
www.elsevier.com/locate/mee

Experimental investigation of fabrication properties of electroformed Ni-based micro mould inserts

Chao-Min Cheng *, Ren-Haw Chen

Department of Mechanical Engineering, National Chiao Tung University, Hsinchu 30010, Taiwan

Received 13 May 2004; received in revised form 17 June 2004; accepted 20 July 2004
Available online 12 August 2004

Abstract

In this work, Ni and Ni–Fe micro mould inserts with high aspect ratios are fabricated by Si–LIGA. Many analyses were performed to elucidate the material properties of Ni-based micro mould inserts. The surface properties were examined using a scanning probe microscope (SPM). Nanoindentation was used to measure the elastic modulus and hardness of Ni–Fe microstructures. When the iron content of Ni–Fe micro mould inserts exceeded 12%, the grain size of the Ni–Fe alloy was under 15 nm. Additionally, the mechanical properties of Ni-based microstructures obtained by electroforming are superior to those obtained by casting or powder metallurgy. Satisfactory electroforming current densities for obtaining a mould insert with a fine surface profile ranged from 4 ASD to 6 ASD.

Keywords: Electroforming; SIGA; Micro mould insert; SPM; Nanoindentation

1. Introduction

The LIGA process is one of the main methods of fabricating microstructures, especially those with high aspect ratios. However, synchrotron radiation is hard to obtain; the cost of X-ray masking is high and the process of fabrication is very complex [1]. Therefore, a LIGA-like process that involves altered processes is inevitable. Unlike the standard LIGA process, the SIGA (**Si**lizium-Mikrostruktur, **G**alvanik und **A**bformung; Silicon Microstructure, Electroforming and Micromoulding) process evolved from the standard Si-process is very compatible with the integrated circuit process and the equipment required is simpler than that required by the LIGA process [2,3]. Moreover, microcomponents made of metallic alloys can be produced using the LIGA or SIGA method. They are used as sensors or actuators, or more generally, as parts of microelectromechanical systems.

* Corresponding author. Present address: B205B, Institute of Physics, Academia Sinica, Nankang, Taipei, 11529, Taiwan. Tel.: +886 2 27880058x4052; fax: +886 2 27834187.
E-mail address: cmcheng@phys.sinica.edu.tw (C.-M. Cheng).

0167-9317/$ - see front matter
doi:10.1016/j.mee.2004.07.066

In this work, the silicon-based master is fabricated by anisotropic etching and thick-film lithography; the Ni-based materials are then electroformed on the silicon-based master. Several studies have addressed the electroforming of micro mould inserts as part of LIGA (or SIGA) [4–9]. However, relatively few studies have measured and reported values of elastic modulus, surface roughness and hardness of electroformed Ni and Ni–Fe microstructures [10,11]. Furthermore, the mechanical and surface properties of micro mould inserts influence strongly the micromoulding process, so these properties must be understood.

The development of scanning tunneling microscopy (STM) by Binnig and Rohrer in 1981, led to various forms of scanning probe microscopy (SPM). A small probe was employed to measure the local properties of a sample. Probes have been developed to detect thermal, electrical, magnetic, mechanical and optical properties on the nanometer scale. All forms of SPM require that the probe be close to the sample. The benefit of the SPM technique in MEMS applications is that it proceeds more quickly than standard tensile and hardness testing. Accordingly, the Ni-based microstructures obtained under various electroforming conditions are directly measured and analyzed by scanning probe microscopy (SPM) to elucidate the mechanical and surface properties of the micro mould inserts herein.

2. Fabricating the silicon-based master

All experiments were performed using ⟨1 0 0⟩-oriented, 4-in. p-doped (1–100 Ωcm) silicon wafers. Fig. 1 presents the SIGA process. The silicon-based masters could be fabricated by three various methods individually: wet anisotropic etching, dry anisotropic etching or thick-film lithography. The fabricating processes and properties of the silicon-based master are described below.

2.1. Wet anisotropic etching

A masking layer of thermal oxide with a thickness of 0.6 μm was used for passivation. Arrays of square elements with 50×50 μm were patterned in an SiO_2 mask by ordinary photolithography to evaluate the surface roughness and rate of KOH etching of the (1 0 0) plane. The etching windows were formed by removing SiO_2 using buffered hydrofluoric acid (BOE) solution. The KOH etchant used here was a 25 wt% aqueous solution without added isopropyl alcohol (IPA). The etching experiments were conducted with an etching temperature of 60–100 °C.

2.2. Dry anisotropic etching

After the masking layer was deposited, a photoresist was coated and lithography applied to define the pattern on the masking layer. Then, inductively coupled plasma reactive ion etching (ICP–RIE) was used to etch the single-crystal silicon. In this work, the etching gas was SF_6 and the passivation gas was C_4F_8. Two etching masks, a photoresist and silicon dioxide, were employed. More residues were obtained when the photoresist was used as the etching mask; this problem could be solved by increasing the amount of reactive etching gas. Furthermore, in narrow openings, uneven sidewall profiles were generated because etching and passivation gas exchange were repeated. The flow ratio and period of the etching and passivation gases, and the oxygen inflow could be altered to solve the problem of uneven surface and residues, as indicated in Fig. 2.

2.3. Thick-film lithography

Silicon wafers were cleaned in a dilute HF solution ($HF:H_2O = 1:20$) for 2 min and rinsed in deionized water. A 200 nm layer of copper was deposited by sputtering onto the silicon wafer as a seed layer for electroforming before the SU-8 photoresist was coated. An SU-8 photoresist with a thickness of 100 μm was coated on a silicon substrate following initial cleaning. It underwent soft baking, UV-exposure, post-exposure baking and developing processes.

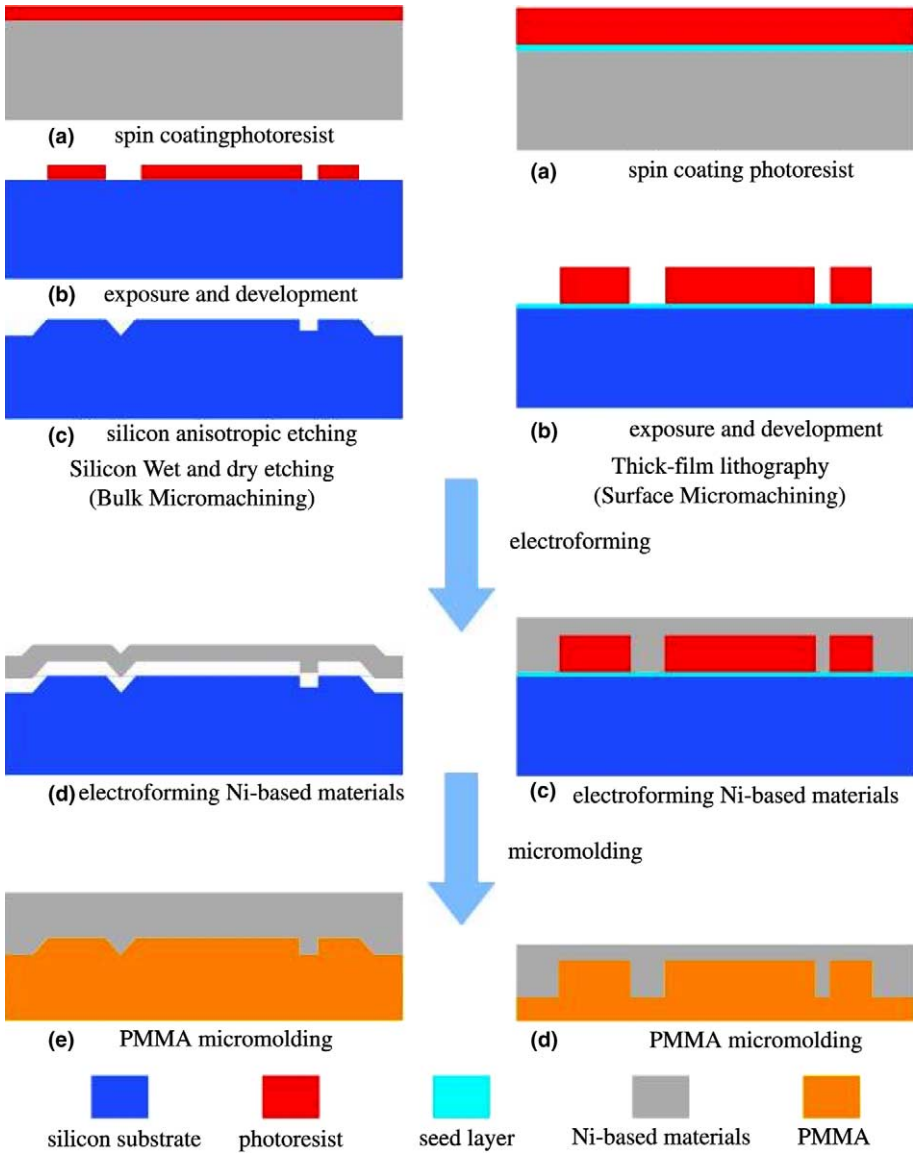

Fig. 1. SIGA (**Si**lizium-Mikrostruktur, **G**alvanik und **A**bformung) fabrication process. Bulk micromachining and thick-film lithography are employed to fabricate silicon-based masters.

2.4. Electroforming Ni-based micro mould inserts

In the SIGA process, the lithographed pattern plate is a three-layer structure. The bottom layer of the three-layer structure is an insulating base plate such as silicon wafer. The middle layer of the three-layer structure is the conductive metal used as a seed layer in electroforming. The top layer of the three-layer structure is the photoresist pattern that has been lithographed. The seed layer for electroforming must has low sheet resistance and strong adhesion to the electroplate metal. The silicon wafer with seed layer formed by sputtering copper or evaporating titanium has a lower sheet resistance and initial current of electroforming than that deposited with other metals, so the

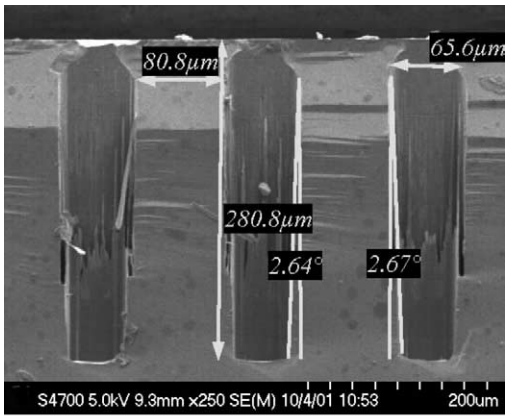

(a)

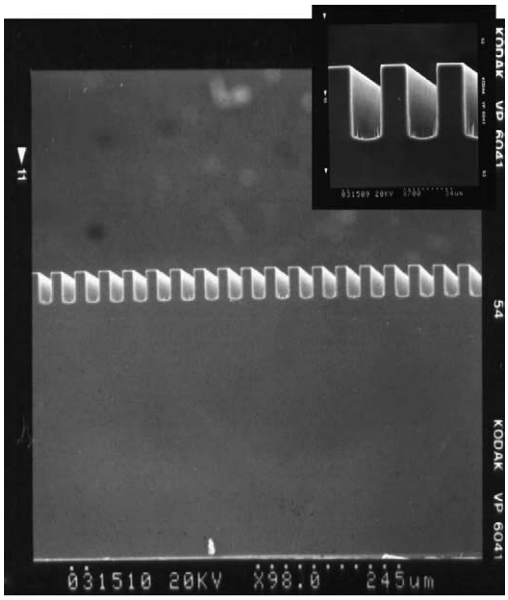

(b)

Fig. 2. SEM micrograph of silicon microstructures fabricated by inductively coupled plasma reactive ion etching (ICP-RIE). The etching mask is silicon dioxide and the etching rate is 3 μm/min. (a) Aspect ratio of silicon deep holes is 4.3 and the taper angles are 2.64 ± 0.03°. (b) Aspect ratio of silicon microchannels is 2.5.

processes of sputtering copper or evaporating titanium are extensively used [1]. Ni and Ni–Fe alloys could be electroformed on a silicon-based master, following wet etching, dry etching and the thick-film lithography. Tables 1 and 2 list the electroforming solutions used in the electroforming of Ni and Ni–Fe alloy. Boric acid was employed to

Table 1
Composition of Ni electroforming solution and conditions of electroforming

Description	Concentration
Nickel sulfamate	420 ml/L
Boric acid	40 g/L
Saccharin	1 g/L
Sodium lauryl sulfate	2 ml/L
Current density	1–5 ASD
pH	3.8–5.2
Temperature	50 °C

Table 2
Composition of Ni–Fe alloy electroforming solution and conditions of electroforming

Description	Concentration
Nickel sulfate	200 g/L
Iron sulfate	8 g/L
Iron chloride	5 g/L
Boric acid	40 g/L
Saccharin	3 g/L
Sodium lauryl sulfate	5 ml/L
Current density	1–5 ASD
pH	2.8–4.5
Temperature	50 °C

stabilize the pH of the electroforming solution, and saccharin reduces the stress between the electroforming layers [12,13]. In the pretreatment prior to electroforming, the plating cell, the rack, the anode basket and the S–Ni anode must clean. Additionally, weak electrolysis must performed at low current density for 12 h to remove metal ions, and an active carbon filter was utilized to filter organic impurities to reduce the number of defects of coating layers, and thus the internal stress of the micro mould inserts could be decreased. Fig. 3 shows some micrographs of electroformed Ni and Ni–Fe alloys. They reveal that the metal was deposited upward following the sidewall of the microstructured photoresist.

3. Quality of electroformed Ni-based micro mould inserts

3.1. Mechanical properties

The metal microstructures were fabricated to serve as micro mould inserts, which must have fine

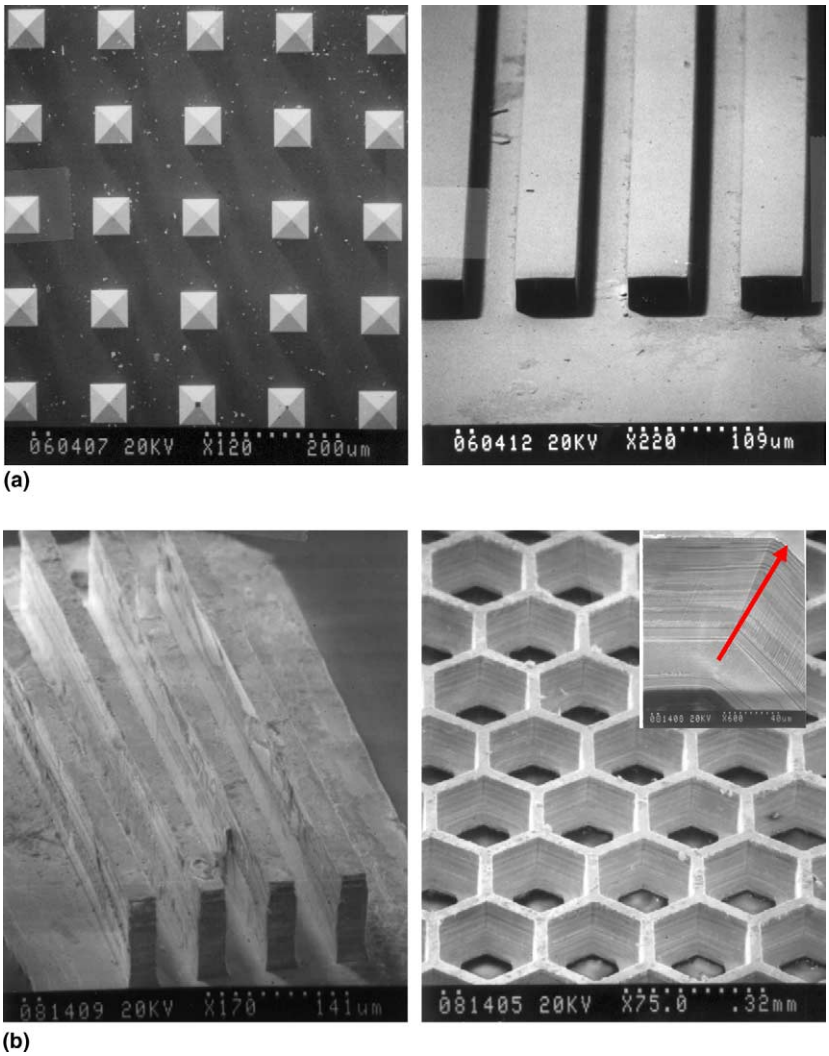

Fig. 3. SEM micrograph of various electroformed Ni-based microstructures. (a) Ni microstructures; micropyramids and microchannels. (b) High aspect ratio Ni–Fe microstructures; microchannels and honey comb microstructures.

mechanical properties. Tensile tests and micro-Vickers hardness tests of the electroformed Ni-based microstructures were conducted; the silicon-based masters of electroformed Ni-based microstructures could be fabricated using thick-film lithography. For comparison, Rockwell hardness tests were performed on the electroformed samples. Fig. 4 plots the tensile stress-strain curves of electroformed Ni and Ni–Fe microstructures using standard tensile tests. The tensile strength of the electroformed Ni–Fe microstructures is 50% higher than that of Ni microstructures. Table 3 compares the mechanical properties of Ni-based products obtained by various processes. This table implies that the mechanical properties – hardness and tensile strength – of metal microstructures obtained by electroforming are superior to those of parts obtained by casting and powder metallurgy.

However, traditional mechanical testing methods, such as standard tensile tests or Rockwell tests, are unsuited to micron/submicron-sized

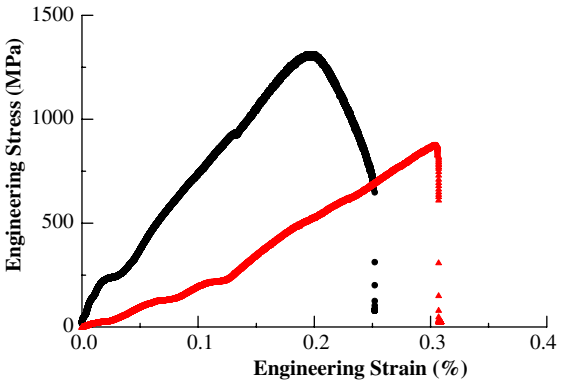

Fig. 4. Stress-strain curve of electroformed Ni and Ni–Fe microstructures. (● Ni–Fe alloy; ▲ Ni; presented result is equalized by several experimental data.)

Table 3
Comparison of mechanical properties of Ni-based products obtained by various methods

	Tensile strength (MPa)	Hardness (HV)	Hardness (HR-B)
Casting parts[a]	420	132.8	–
Powder metalurgy parts[a]	280	75	–
Electroforming microstructures	862 (Ni)	483 (Ni)	98.4 (Ni)
	1274 (Ni–Fe)	541 (Ni–Fe)	> 105 (Ni–Fe)

[a] Engineering Properties of Nickel and Nickel-Alloys, Plenum Press, New York, 1971.

samples, so various studies have been undertaken over the last few years to development a technique for elucidating the mechanical properties of materials on the micron/submicron scale. In this study, the combination of a scanning probe microscope (SPM) and a nanoindenter was employed to visualize microstructures. An indent was then made in the microstructures using a precisely placed indenter tip. The nanoindenter monitored and recorded the load and displacement of a three-sided pyramidal diamond (Berkovich) indenter during indentation with a force resolution of approximately 1 nN and a displacement resolution of about 0.2 nm. After the indentation was made, this indenter tip was used to capture the impression of the indentation on the microstructures. The hardness and elastic modulus were determined from the load-displacement data obtained by nanoindentation.

The electroformed Ni–Fe microstructure was indented by nanoindentation herein. The elastic modulus of an electroformed Ni–Fe microstructure can be evaluated as follows.

$$E_{\text{eff}} = \frac{1}{2}\sqrt{\frac{\pi}{A_c}}\frac{dP}{dh}, \tag{1}$$

$$\frac{1}{E_{\text{eff}}} = \frac{1-v^2}{E} + \frac{1-v_i^2}{E_i}. \tag{2}$$

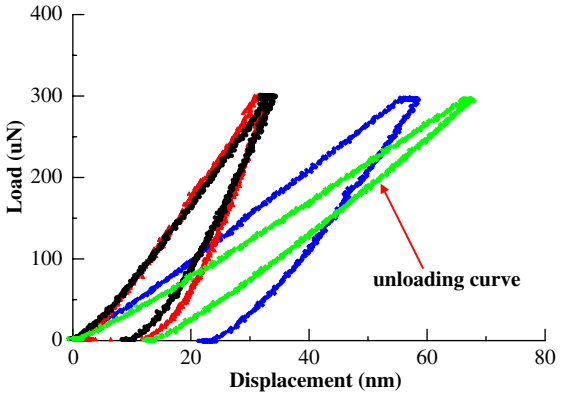

Fig. 5. Nanoindentation load-depth curves (force curves) of electroformed Ni–Fe microstructures at various current densities. (Current densities in electroforming process: ‡ 0.25 ASD, ◆ 0.5 ASD, ● 2 ASD, ▲ 4 ASD.)

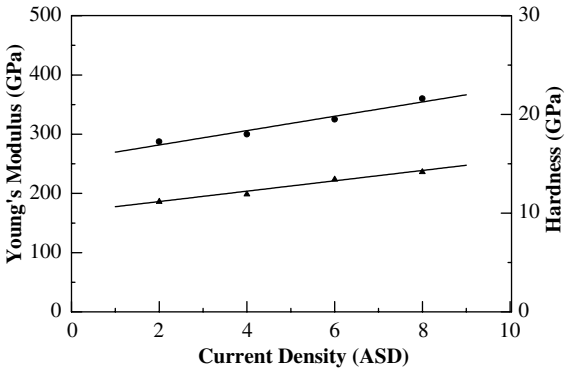

Fig. 6. Effect of current density in the electroforming process on the Young's modulus and hardness of electroformed Ni–Fe microstructures. (● Young's modulus; ▲ hardness; presented result is equalized by several experimental data.)

Here, $\frac{dP}{dh}$ is the experimentally determined stiffness of the upper part of the unloading data, as indicated in Fig. 5; E_{eff} is the reduced modulus (previously defined) and A_c is the projected area of elastic contact. The modulus can thus be derived by measuring the initial unloading stiffness and assuming that the contact area equals the optically measured area of the impression [14,15]. The parameters E and v are the elastic modulus and Poisson's ratio of the specimen and E_i and v_i are those of the indenter, which are 1141 GPa and 0.07, respectively. The Poisson's ratio of the electroformed Ni–Fe microstructures is 0.27 here.

Fig. 6 plots the influence of the electroforming current density on the Young's modulus and hardness of the electroformed Ni–Fe microstructures. The figure demonstrates that the elastic modulus and the hardness increase with the current density, perhaps because increasing the current density increases the rate of reduction of metal ions at the cathode yielding finer grains of the electroformed metal, which is thus strengthened. Additionally,

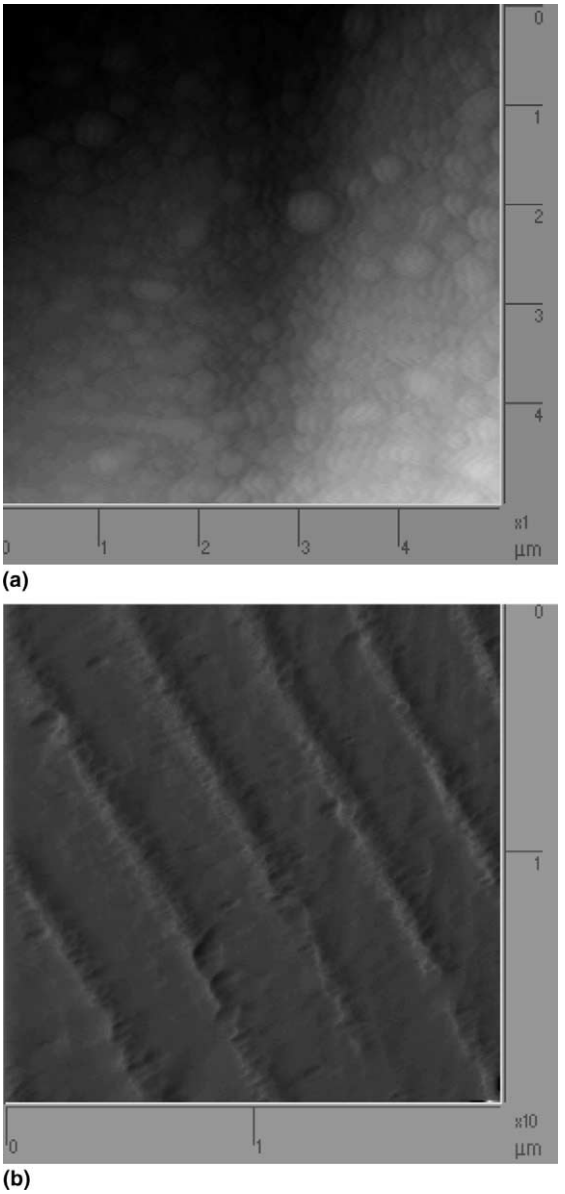

Fig. 7. Analysis by scanning probe microscopy (SPM) of electroformed Ni microstructures. (a) Grain size of electroformed Ni. (b) RMS transformation of (a).

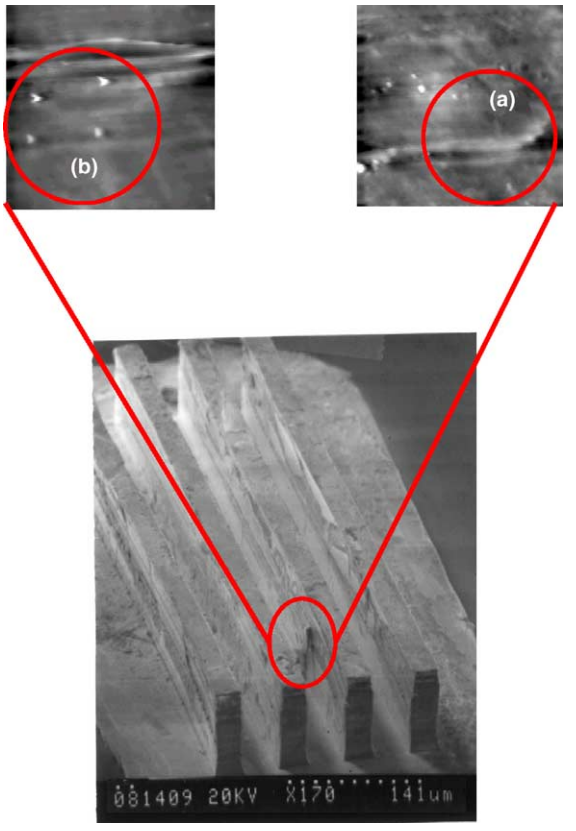

Fig. 8. SPM analysis of electroformed Ni–Fe microstructures. Defects on the lateral side of the microstructure are observed and analyzed directly using SPM.

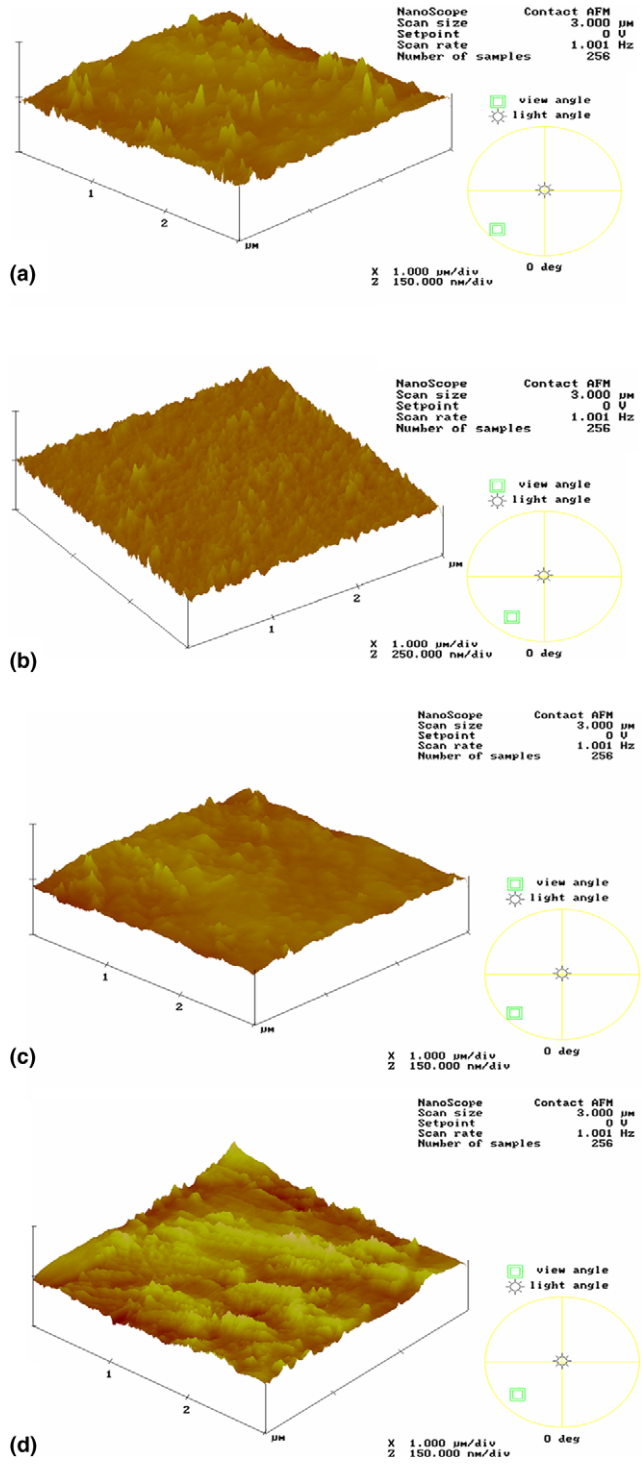

Fig. 9. SPM images of electroformed Ni–Fe microstructures obtained at various current densities. (a) 2 ASD; (b) 4 ASD; (c) 6 ASD; (d) 8 ASD.

increasing the current density can also increase the fraction of iron precipitated, increasing the hardness. Moreover, a high current density induces the formation of Ni–Fe alloy with a (1 1 1) preferred crystallographic orientation, increasing its hardness. In fact, in this work, when the iron content of the electroformed Ni–Fe alloy, measured by using electron probe microanalysis (EMPA), exceeded 12%, the grains of the electroformed Ni–Fe microstructures were smaller than 15 nm and the elastic modulus could be as high as 316 GPa according to a qualitative analysis.

3.2. Surface properties

The surface properties of Ni-based micro mould inserts directly influence the demoulding properties and the quality of the moulded polymer microstructures. Herein, a scanning probe microscope (SPM) was used to elucidate the topography of the Ni-based micro mould inserts. Fig. 7(a) displays SPM images of the electroformed Ni microstructures. The sizes of the grains of electroformed Ni microstructures are observed directly to be several sub-microns – smaller than those of Ni parts manufactured by casting or powder metallurgy. The actual features of the surface of a microstructure can be obtained by root mean square (RMS) transformation, as shown in Fig. 7(b). According to the Hall–Petch equation

$$\sigma_y = \sigma_0 + k_y d^{-1/2}, \tag{3}$$

where σ_y is the yield strength, d is the average grain diameter, and σ_0 and k are constants for a particular material [16]. Therefore, the mechanical strength of the microstructures obtained by electroforming is greater than that obtained by casting or powder metallurgy. Maintaining cleanliness and sharpness of the tip is very important because these factors influence the resolution of the images.

The defects in electroformed Ni–Fe microstructures were observed directly by SPM, and are presented in Fig. 8. This figure reveals that the cracks in the microstructure are perpendicular to the direction of deposition of the metal because other species are present in the deposited metal during electroforming. The microbubbles of hydrogen can result in a non-uniform surface profile during electroforming, as indicated in Fig. 8(b) (triangular regions). Hence, quickly excluding hydrogen is a key to improving the condition of the surface profile during the electroforming of microstructures with high aspect ratios. Demagnetization is important for performing this experiment because Ni–Fe alloy is a magnetic material and magnetism strongly affects scanning. Fig. 9 present the topographic map, elucidated by SPM, of Ni–Fe microstructures electroformed at various current densities. This figure reveals that a fine surface profile, which is favorable for mould inserts, can be obtained when the density of the electroforming current is between 4 ASD and 6 ASD.

4. Summary

This work investigated Ni and Ni–Fe microstructures produced using the SIGA process. Tests were conducted on mechanical properties to determine parameters such as elastic modulus, tensile strength and hardness, which were compared with corresponding values for nickel parts formed by casting and powder metallurgy. The results show that the mechanical properties of microstructures obtained by electroforming are superior to those of microstructures formed by casting or powder metallurgy; the tensile strength of the former can be up to 1274 MPa. Also, the elastic modulus of Ni–Fe microstructures was determined by nanoindentation and the elastic modulus increased with the density of the electroforming current. With regard to the surface properties of the Ni-based microstructures, the grain size and surface conditions were observed directly by scanning probe microscopy. The observations indicate that the size of grains in electroformed Ni microstructures can be up to several tens of nanometers; however, the fine surface profiles of Ni–Fe microstructures were obtained at current densities of between 4 ASD and 6 ASD.

Acknowledgements

The authors thank Dr. Y.-M. Yeh of the Department of Vehicle Engineering, Chung Cheng Institute of Technology, National Defense

University, Taiwan, for many fruitful discussions. We also thank the Semiconductor Research Center (SRC) of National Chiao Tung University, Hsinchu, Taiwan, for providing equipment.

References

[1] M.J. Madou, Fundamentals of Microfabrication, second ed., CRC Press, New York, 2002.
[2] R. Klein, A. Neyer, Electron. Lett. 30 (1994) 1672–1674.
[3] S. Kalveram, A. Neyer, SPIE 3135 (1997) 2–11.
[4] H. Majjad, S. Basrour, P. Delobelle, M. Schmidt, Sensor Actuator A 74 (1999) 148–151.
[5] S. Abel, H. Freimuth, H. Lehr, H. Mensinger, J. Micromech. Microeng. 4 (1994) 47–54.
[6] W. Daniau, S. Ballandras, L. Kubat, J. Hardin, G. Martin, S. Basrour, J. Micromech. Microeng. 5 (1995) 270–275.
[7] J. Fahrenberg, T. Schaller, W. Bacher, A. El-Kholi, W.K. Schomburg, Microsystem Technol. 2 (1996) 174–177.
[8] S. Roth, L. Dellmann, G.-A. Racine, N.F. de Rooij, J. Micromech. Microeng. 9 (1999) 105–108.
[9] L.S. Stephens, K.W. Kelly, S. Simhadri, A.B. McCandless, E.I. Meletis, J. Microelectromech. Systems 10 (2001) 347–359.
[10] E. Mazza, S. Abel, J. Dual, Microsystem Technol. 2 (1996) 197–202.
[11] J.T. Ravnkilde, V. Ziebart, O. Hansen, H. Baltes, Sensor Mater. 12 (2000) 99–108.
[12] R.-H. Chen, C.-C. Chang, C.-M. Cheng, Fabricating a micro mould insert using a novel process, Int. J. Adv. Manufac. Technol., in press (2003).
[13] Y.-M. Yeh, G.-C. Tu, T.-H. Fang, Nanomechanical properties of nanocrystalline Ni–Fe mold insert, J. Alloys Compd. 372 (2004) 1564–1583.
[14] W.C. Oliver, G.M. Pharr, J. Mater. Res. 7 (1992) 1564–1583.
[15] X. Li, H. Gao, C.J. Murphy, K.K. Caswell, Nano Lett. 3 (2003) 1495–1498.
[16] R.E. Reed-Hill, R. Abbaschian, PWS Publishing Company, Boston, 1973.